Fuel Cells

Synchrotron Radiography for a Proton Exchange Membrane (PEM) Electrolyzer

Journal:	*Fuel Cells*
Manuscript ID	fuce.201900055.R2
Wiley - Manuscript type:	Original Research Paper
Date Submitted by the Author:	n/a
Complete List of Authors:	Panchenko, Ulla; Forschungszentrum Jülich Institut für Energie- und Klimaforschung, Arlt, Tobias; Technische Universität Berlin, Institue of Material Science and Technology Manke, Ingo; Technische Universität Berlin, Institue of Material Science and Technology Müller, Martin; Forschungszentrum Jülich GmbH, IEK-3, Electrochemical Process Engineering Lehnert, Werner; Forschungszentrum Juelich GmbH, IEK-3: Electrochemical Process Engineering Stolten, Detlef; Forschungszentrum Jülich GmbH, IEK-3 Electrochemical Process Engineering
Keywords:	synchrotron radiography, PEM electrolysis, two-phase flow, catalyst layer degradation, blistering in porous materials

Synchrotron Radiography for a Proton Exchange Membrane (PEM) Electrolyzer

U. Panchenko,[1] T. Arlt,[2] I. Manke,[3] M. Müller,[1,*] D. Stolten[1,4] and W. Lehnert[1,5]

[1] Institute of Energy and Climate Research

Electrochemical Process Engineering (IEK-3), Forschungszentrum Jülich GmbH, Jülich, Germany

[2] Technische Universität Berlin, Insitute for Materials Science, Berlin, Germany

[3] Institute of Applied Materials, Helmholtz-Zentrum Berlin, Berlin, Germany

[4] Chair for Fuel Cells, RWTH Aachen University, Aachen, Germany

[5] Faculty of Mechanical Engineering, RWTH Aachen University, Aachen, Germany

[*]Corresponding author: mar.mueller@fz-juelich.de

Abstract

In-plane synchrotron radiography with a resolution of a few micrometres was applied to study transport processes within a Proton Exchange Membrane (PEM) electrolyser cell. The degradation process of the catalyst layer, gas production with bubble formation at the catalyst layer and in the porous transport layer (PTL) was analysed. From this, a new cell design was developed that allows for high X-ray transmittances at the membrane plane in the in-plane viewing direction. During the measurement, a bubble growth and movement was observed. Furthermore, a detachment of catalytic material from the catalyst layer was detected. Afterwards, a post-mortem EDX analysis was conducted to determine the position of the catalyst particles. Despite Iridium being initially used as the anode catalyst and platinum as the cathode catalyst, the EDX measurement revealed Pt and Ir particles on both electrodes following cell operation.

Keywords: Synchrotron radiography, PEM electrolysis, two-phase flow, catalyst layer degradation, blistering in porous materials

1 Introduction

Electrolysis is an important component in the transition of the energy system towards a renewable basis. One application of electrolysis is the power-to-gas concept, in which chemically-bound energy is released as electrical energy. Energy production with solar installations and wind turbines is highly dependent on the weather, which can be compensated by storing excess energy in the form of hydrogen.

In an electrolysis cell, water is added and gas is produced: oxygen on the anode side and hydrogen on the cathode side. It is a two-phase flow with gaseous hydrogen, water vapor and liquid water. System characterization and description is further complicated because this two-phase flow occurs in a porous material, namely a porous transport layer (PTL). The PTL is essential for homogeneous water distribution and efficient gas discharge. Such layers are frequently porous structures sintered from titanium powder or made of titanium mesh.

Gas produced in the form of bubbles can partially cover the catalyst and impede the access of the water to the catalyst and thus hinder the electrochemical reaction. Such gas accumulations are also called mass transport limitations and can cause overpotentials which have to be avoided. The aim is to better understand ~~bubble~~ multi-phase transport in the titanium based PTL and thus ensure efficient gas discharge. The investigation of ~~blistering~~ the bubble formation becomes difficult, as it takes place in the small pores of a porous medium and a high local resolution is neccessary. The solution to this is the use of synchrotron radiography, which allows for very good contrast between water and gas in the pores of the PTL.

Mass transport limitations and overpotentials have been investigated by Roy et al. [1]. Selamet et al. [2] use soft X-ray radiography to visualize the behavior of gas bubbles. The in-plane measurement shows how the gas bubbles first develop in the PTL in different operating modes, then grow to the PTL surface and are finally discharged. Leonard et al. [3] use X-ray computed tomography (CT) and radiography in parallel to study morphology, oxygen bubble formation and bubble removal under PEM electrolyzer operating conditions. In other studies,

synchrotron radiography was used and blistering between the land and channel of an electrolysis cell was observed [4, 5]. Bubble size and the growth cycle were also investigated depending on the operating points. Markötter et al. [6] combined synchrotron radiography and synchrotron tomography to investigate the water distribution in the PTL of a fuel cell. In case of fuel cells the porous transport layers are usually made of graphite fibers. Monochromatic synchrotron radiation is also well-suited to analyses of the degradation processes of catalyst layers [7, 8]. These effects can also be analyzed on a smaller scale by combining synchrotron radiography and focused ion beam tomography [9]. Hinebaugh and Lee et al. [10, 11] used synchrotron radiation to investigate water percolation in the porous layers of a fuel cell. Droplet formation and propagation were visualized.

According to conventional concepts, the gas bubble forms directly at the catalyst. Lubetkin et al. [12] showed that when the gas concentration in a water solution exceeds a critical limit, gas bubbles form in the liquid or on the PTL surface. Interfacial strain, the contact angle and oversaturation determine whether the bubbles form on the catalyst surface or in the PTL pores. In order to maintain water electrolysis, water must first diffuse to the catalyst surface. The reaction on the catalyst surface can then proceed faster than the transport of the reactants. A study by Chen et al. [13] showed that the time of bubble formation does not depend on the operating point (e.g., current density), but rather on the concentration of the gas dissolved in the water at the surface of a catalyst. The surface roughness also influences the process of gas bubble growth and detachment. Catalysts with a higher surface roughness lead to faster bubble detachment and thus reduce the bubble size [14]. Some studies [15, 16] have shown that bubble formation improves mass transport. Bubbles in the channel increase PTL through-flow. Lee et al. [17] observed a change in gas distribution in the PTL from the catalyst-coated membrane (CCM) to the channel. At the CCM, fairly smaller bubbles are present. In the direction of the canal, individual transport paths grow together and larger bubbles are observed.

Next, we wanted to investigate catalyst degradation, as the in-plane measurement allows visualization of catalyst separation and movement in the PTL pores.

The cathode catalyst is usually made of carbon-supported platinum particles. The aging and degradation processes discussed in the literature point to the reduction of the available ~~electrochemically-active~~electrochemically active platinum surface (ECSA). The platinum particles migrate and ~~-~~reducing the ECSA. The consequence of this platinum migration is local de-passivation of the surface caused by place exchange processes in the catalyst layer. In case of ~~a~~ fuel cells ~~T~~this is caused by oxide formation and oxide reduction along with molecular oxygen evolution in addition to the Platinum dissolution~~.~~ [18]. In PEM electrolysis ~~Another~~additional degradation processes occur, the increase of contact resistance and the associated loss of performance is described in [19] and on the other hand particle agglomeration known as Ostwald ripening, causes agglomerates to grow larger, as small agglomerates get smaller and disappears [20]. ~~-~~Catalyst particles are usually sintering together to agglomerates of a number of catalyst particles, reducing the surface area to volume ratio of the particles in each case. This mainly occurs at the high potential at the cathode of a PEM fuel cell. In the cathode of the PEM electrolyzer, the potentials are much lower and degradation would be expected to be much less severe. But particles detach from the carrier and lose electrical contact with the electrode, in which case the catalyst particle is no longer available for catalysis.

LaConti et al. [21] provide an overview of studies on membrane degradation in fuel cells in the last 30 years and compare it with electrolysis. The authors distinguish between chemical and mechanical influences on membrane degradation. Mechanical stress factors include thermal membrane expansion, as well as membrane damage from the PTL surface. Chemical stress is caused by the formation of peroxyl radicals, which attack the membrane. A higher temperature accelerates the chemical degradation processes.

Grigoriev et al. [22] describe a degradation mechanism in the electrolysis cell in which the platinum diffuses through the membrane. This aging phenomenon is known in the PEM literature as *platinum ribbon*. Debe et al. [23] demonstrated the platinum particles used as the cathode catalyst on the anode side after 1500 hours of operation. Iridium diffuses from the anode to the cathode side, with the anode catalyst layer showing a crystallite enlargement of 40%. As a conclusion of the elemental analysis, two migration processes were suspected. The anode catalyst (Ir) diffuses to the cathode side and the cathode catalyst (Pt) to the anode side, i. There is a catalyst migration in each opposing direction. However, the element detection in the membrane (platinum ribbon) was not carried out. Feng et al. summarize the degradation phenomena of PEM electrolysis and offer an idea of what future research trends could be [24].

As ~~W~~we have already performed tests with neutron radiography at the beamline at Helmholtz Center Berlin [25] ~~and~~ we have found that the spatial resolution of this device is limited to around ~~-~~6.3~~-~~ µm. We also now about the higher resolution of other neutron sources, for an example up to 1.5 µm at the NIST [26] but due to the limited availability~~Therefore I~~in this study, synchrotron X-ray radiographic imaging was employed to dynamically visualize the bubble formation and catalyst degradation. With a combination of synchrotron radiography and in-plane measurement, it is possible to study not only bubble formation as a function of operating conditions, but also the propagation of bubbles in the pores of a PTL. We aim to verify the theory of Lubetkin et al. [12] as to whether bubbles form not only on the catalyst surface, but also on the PTL surface, when the super saturation of gas in water has been achieved. We also want to visualize the change in catalyst layer *operando*. Subsequently, the distribution of chemical elements in PTL is investigated *postmortem*.

2 Experimental

To experimentally investigate the gas-water transport *operando*, an electrolysis cell suitable for synchrotron radiography was designed (Figure 1). In-plane measurement was then used to investigate gas production and transport inside the PTL and the degradation processes at the boundary between the CCM and PTL. Due to the limited penetration depth of the synchrotron beam and strong absorption by the titanium material, as little material as possible should be located in the beam direction (see Figure 1 a) gives the view from the side and b) gives the front view.). This challenge was resolved by contacting the CCM on both sides, not with the surfaces of two sintered bodies, but rather with their lateral edges. Water was supplied to both the anode and cathode, so that one could observe the two-phase flow on both sides (cathode and anode).

The electrolysis cell was assembled with a PTL sample made from shapeless, sintered titanium particles fabricated using the hydride-dehydride (HDH) process, with a particle fraction below 45 µm. The sample thickness was 1200 µm and its porosity was 45%. Pore size distribution was measured by mercury porosimetry. Pore radius ~~is logarithmic and~~ is logarithmic normal distributed ~~normally distributed~~ with the peak at 6 µm and a Full Width at Half Maximum (FWHM) of 4 µm. Only 0.5 % of all pores are larger than 10 µm. But if you look at pore volumes, 0.5 % pores make up 99.6 % of all pore volumes. As an example, there are only 0.0006 % of pores around 100 µm in size, but they form almost 40 % pore volume. Each sintered body part had dimensions of 10 x 4.5 x 1.2 mm^3, with an active surface of 10 x 1.2 mm^2.

In the experiment, we used home-made CCMs that were made using the decal process. A Nafion membrane coated with a catalyst was also used. This was the Nafion N117 membrane from DuPont, with an iridium loading of 2.2 mg cm^{-2} and a platinum loading of 0.8 mg cm^{-2}. Each end plate of the cell had two water connections on opposite sides, a depression for the PTL and CCM, two distribution channels to homogeneously distribute the water and holes to

bolt the cell together with a torque of 5 Nm. Two sintered bodies also contacted the CCM with their lateral edge. The CCM was inserted between two sintered bodies in an "S"-like shape. Metal pins were then used to guarantee electrical contact. Such metal contact pins have threads and are screwed into the cell. While inserting the contact pins, the PTL plates were also pressed together. Contact pins were used by hand, and it cannot be said what force the PTL and CCM printed together. In order to minimize the thickness of the Plexiglas in the beam path, depressions of 5 x 5 mm^2 were also milled into both end plates. The Plexiglas end plate thickness was 2.5 mm in the beam direction. As the cell end plates were made of Plexiglas, there was no possibility of heating the cell. The cells were therefore operated at room temperature.

The radiographic measurements were performed at BAMline at the Helmholtz Center in Berlin, Germany [27]. According to the specifications of the camera used during the synchrotron measurement, structures in the range of about 0.5 µm can be resolved within a field of view of 1.7 x 1.2 mm^2 (4008 x 2672 pixels). The specified resolution is checked with a Siemens Star device so that we are sure the ~~S~~structures of a few µm in size can indeed be distinguished ~~in this way~~. The camera model was a pco4000 combined with a 20 µm Gadox scintillator. The temporal resolution was 2 seconds. During the measurement, the beam energy was adjusted to 16 keV and Al 0.5 mm and Be 0.5 mm metal filters were used to form the synchrotron beam.

The synchrotron beam loses intensity when passing the cell, as intensity is absorbed by the cell components. The part of the beam that is not absorbed is detected as the transmitted intensity. The Lambert-Beer law outlines how the beam intensity is attenuated during transmission through the material. The attenuation depends exponentially on the material attenuation coefficient and the material thickness:

$$I_t = I_0 \cdot e^{-\sum \mu \cdot z} \quad (1)$$

where I_0 is the original beam intensity, I_t is the transmitted intensity, μ is the mass attenuation coefficient and z is the material thickness.

In practice, an image or image series with a defined state of the cell is required, e.g., a completely wet or dry cell. For the following analyzes, all other images are divided by this normalization (completely wet) image.

$$I_w = I_0 \cdot e^{-(\mu_w z_w + \mu_p z_p)} \quad (2)$$

$$I_d = I_0 \cdot e^{-(\mu_w z_d + \mu_p z_p)} \quad (3)$$

where I_w is the beam intensity of a completely wet state, I_d is the beam intensity of the other "dry" state, μ_w is the mass attenuation coefficient of water and z_w is the water thickness, while μ_p is the mass attenuation coefficient of Plexiglas and z_p the Plexiglas thickness.

If we divide equation (2) by equation (3), many unknown parameters will be truncated.

$$I_w / I_d = e^{-\mu_w (z_w - z_d)} \quad (4)$$

$$(z_w - z_d) = -\frac{1}{\mu} ln\left(I_w / I_d\right) \quad (5)$$

$(z_w - z_d)$ presents the gas fraction that has displaced the water. Further image processing follows in accordance with the Lambert-Beer law; the images produced by normalization of the logarithm of the radiation's intensity relation was taken for all images. Subsequently, these images were divided by the attenuation coefficient of water, which is about $\mu = 0.11$ mm^{-1} for E = 16 keV. The result describes the two-dimensional information of the gas thickness in the beam direction inside the operating electrolyzer.

Energy-dispersive X-ray spectroscopy (EDX) was used to characterize the elemental composition of the observed sample areas. An X-ray diffractometer, a Bruker D8 DISCOVER with Cu TWIST-TUBE X-RAY SOURCE, was used. With this, an electron beam is focused and driven line by line over the surface. The beam electron precipitates from the sample of

one of the near-nuclear electrons in an atom. One of the higher-energy electrons reaches this energetically more favorable level, while the energy difference is released as an X-ray quantum. The detector detects the energy of the X-ray quantum, which is characteristic of a chemical element. When scanning the surface with these methods, it is possible to detect the distribution of chemical elements.

3 Results and Discussion

The high resolution of synchrotron radiography allowed the calculation of not only the mean volume of water or gas, but also the capacity to visualize the formation and movement of individual gas bubbles in the PTL.

3.1 Bubble formation

Figure 2- a) shows a picture of the cell *operando*. In the middle image area is the CCM, and from both the anode and cathode sides, the PTL can be seen. The PTL range is darker because titanium absorbs more beam intensity than the thin CCM, with a total thickness of about 333 µm. The cathodic catalyst layer can be identified as a dark structure with a thickness of 56 µm. According to the pictures, the membrane does not seem to be in contact with the cathode PTL. The polarization curves show, however, that the electrochemical reaction has taken place (see Figure 2 ~~b~~c). The processed images also show gas bubble production, confirming the normal functioning of the cell. The length of the contact surface is 10 mm, with the field of view of the camera being only 1.2 mm, hence just over 10% is detected. The gap between the CCM and cathodic flow structure is about 500 µm-wide and the contours are not clearly recognizable, which is caused by the fabrication of the PTL, e.g., when cutting the PTL with a water jet. The CCM and PTL make contact outside the field of view of the camera.

The synchrotron radiography images show a very good resolution and structures of a few microns can be distinguished.

After image processing, static "objects" such as the pores of material are filtered out and moving "objects" such as catalyst particles and gas bubbles become visible. The pictures show changes in the cathode PTL during the recording of a polarization curve.

Figure 2 c) to 2 e) ~~to e)~~ showsing bubble growth and transport in the PTL at a current density of 0.1 A cm^{-2}. A section of the PTL can be seen on the cathode side. This means that gas is produced on the right and transported away to the left with the flow. For a better identification of bubbles, the interesting structures are bordered with colored lines. One also observes elongated, rectangular particles, up to 10 µm in length, that absorb much radiation and therefore appear dark. It is the cathode catalyst (platinum).

The image series shows how the bubbles grow and slowly fill the pores so that the shape and configuration of the pores becomes visible. In the image at 62 s, three bubbles can be seen that fill neighboring pores in the beam direction. Superimposed bubble contours indicate that these effects are not surface effects, but are related to gas transport in the volume.

Pores that became visible through the gas bubbles have diameters of 0.1 to 0.2 mm.

The mercury porosimetry shows a mean pore radius of 6 µm with a lognormal distribution, see Figure 6. Thus, there is a smaller percentage of big pores. There are two reasons why only large pores are visible: First, because Titan PTL is hydrophilic, the bubbles prefer to use large pores for transport; second, because of smaller size, it is difficult to sharply resolve the small pores. Presumably, the small pores that are filled with gas that appears as image noise.

It was also observed that the bubbles consistently use the same pore network, and that bubble movement through the connected pores is repeated in the time interval. Preferred pathways exist for gas transport in the PTL. As the current density increases, more hydrogen bubbles can be seen. The movement of bubbles through the pore network increases in speed. Increasing gas production then opens up new "pore pathways".

This images shows how the bubble in the PTL structure grows at a certain distance to the catalyst. It is not clear, however, whether this is the effect described by Lubetkin [8] or if the gas is directed from the catalyst layer through a micropore that is not visible at this resolution. As the bubbles grow, the contours of several connections with neighboring pores simultaneously become visible, thus making alternative pathways for further bubble propagation visible. As can be seen in the image at 86 sec., the bubble grows and spreads and then two neighboring pore throats simultaneously become visible. After a few seconds, the bubble spreads into one of the two neighboring pores. The pressure builds up and the bubble expands through the widened-in-its-circumference pore neck. This process is known as "one-throat-at-a-time" [28]. The limiting pore necks have a decisive influence on the gas balance and the pressure gradient in the PTL.

3.2 Degradation of the anodic catalyst layer

During the first test, strong degradation and detachment of the anode catalyst layer was observed. Before the measurement with the synchrotron beam, the cell was wetted with water for 30 minutes. A polarization curve was then recorded. The cell was observed using the synchrotron beam during humidification and operation. However, catalyst removal only became visible with the operation of the cell. This excludes the synchrotron beam as a factor in the catalyst removal.

The current density was increased in steps of 0.1 A cm^{-2} every 10 minutes up to 0.6 A cm^{-2}. At such low current densities, the cell has already reached a voltage of 2.2 V, and so the current has not been increased further. The -polarization plot (see Figure ~~2b~~5) indicates the influence of the water flow rate on the performance. The cell operates stable only at the low flow rate (0.1 ml min^{-1}) the performance drops down a little bit. -Figure 3 shows the image series depicting the catalyst degradation.

The CCM, which is contacted on both sides by the PTL, can be seen vertically in the center of the image. At the first operating point with no current, no catalyst degradation was observed (Figure 3a). When the current was switched on, some particles moved within the catalyst layer (Figure 3b). The subsequent images (c-e) show how ever more small particles, as well as larger agglomerates with a length of up to 100 µm, detached from the catalyst layer and moved towards the anode side. This degradation process is not dependent on the radiation; otherwise, it would have begun when the measurement started. Rather, this detachment depends on the electrochemical processes and mainly affects the anode catalyst. On the cathode side, a minimal change can be observed in the catalyst layer, but is negligible compared to the anode side. The separated catalyst particles move with the water flow from the CCM to the channel. The type of movement proves that the particles move through the pores of the PTL. The particles tumble to one place, and then move in leaps and bounds. The particles are swirled with the flow into a pore and then carried along to the next one. When assembling the cell, the rubber seal between the PTL and end plate was installed. During pressing, the rubber seal fits into the surface roughness and prevents the formation of a gap. The degradation and detachment process occur within the first hour of operation. After this, no further changes were registered in the catalyst layer. One of the reasons why such severe degradation was observed could be the mechanical stress that the CCM was exposed to when installing in such a non-conventional cell. However, this does not explain why the cathode side is not so heavily affected. Another possible reason for is the decal process that was used in the manufacturing process. A suboptimal adaption of the manufacturing protocol on the geometry of the test cell may be responsible for poor coating adhesion.

3.3 EDX

To determine the distribution of chemical elements in the PTL after the test, the PTL was analyzed by means of EDX. The element distribution on the PTL surface was thus

investigated (Figure 4). To determine the distribution of the elements inside the porous structure, the sintered bodies were subsequently embedded and ground down to the sample center. Then, an EDX analysis of the inner PTL structure was performed. Ir was only present on the anode in the pristine state and Pt only on the cathode after cell operation EDX showed that Pt and Ir are present on both electrodes, on the surface and inside the PTL structure. The cell was in operation for almost 24 hours, which did not explain such strong catalyst degradation. No catalyst inside the membrane was detected, suggesting that the mutual catalyst migration does not pass through the Nafion membrane, but through the imperfections in the seal. The fact that the catalyst particles were also found in the pores of the PTL confirms the movement of the catalyst particles through the pores of the PTL.

4 Conclusions

Synchrotron radiography is a suitable method for visualizing bubble formation and transport in porous structures. The unique and innovative cell design allows for the visualization of bubble formation and transport in the PTL. In this study, individual bubbles that fill the pores and propagate through the PTL were successfully visualized. The gas flow from the CCM to the channel was also observed. When propagating through the PTL, the bubbles used preferred pathways with low flow resistance. With increasing current density, new transport pathways were activated.

Strong particle detachment from the anode catalyst layer was also observed. During a subsequent in-plane synchrotron measurement, the temporal and operating-point dependence of the catalyst detachment was investigated. Catalyst detachment does not depend on the operating conditions and always takes place after the cell has been put into operation. The mutual diffusion of catalysts was also detected, as were Pt and Ir diffusions through the Nafion membrane after such a short operating time (24 hours).

Acknowledgements

The authors would like to thank HZB for granting beam time and numerous technical discussions. Furthermore, financial support within the NeStPEL project, provided by the German Federal Ministry for Economic Affairs and Energy (BMWi, Förderkennzeichen 03ET6044A), is highly appreciated.

References

[1] Roy, A.; Watson, S.; Infield, D., Comparison of electrical energy efficiency of atmospheric and high-pressure electrolysers. *International Journal of Hydrogen Energy* **2006,** *31*, 1964-1979.
[2] Selamet, O. F.; Deevanhxay, P.; Tsushima, S.; Hirai, S., Visualization of Gas Bubble Behavior of a Regenerative Fuel Cell in Electrolysis Mode By Soft X-Ray Radiography. *ECS Transactions* **2013,** *58*, 353-360.
[3] Leonard, E.; Shum, A. D.; Normile, S.; Sabarirajan, D. C.; Yared, D. G.; Xiao, X.; Zenyuk, I. V., Operando X-ray tomography and sub-second radiography for characterizing transport in polymer electrolyte membrane electrolyzer. *Electrochimica Acta* **2018,** *276*, 424-433.
[4] Hoeh, M. A.; Arlt, T.; Manke, I.; Banhart, J.; Fritz, D. L.; Maier, W.; Lehnert, W., In operando synchrotron X-ray radiography studies of polymer electrolyte membrane water electrolyzers. *Electrochemistry Communications* **2015,** *55*, 55-59.
[5] Seweryn, J.; Biesdorf, J.; Schmidt, T. J.; Boillat, P., Communication—Neutron Radiography of the Water/Gas Distribution in the Porous Layers of an Operating Electrolyser. *Journal of The Electrochemical Society* **2016,** *163*, F3009-F3011.
[6] Markötter, H.; Manke, I.; Haußmann, J.; Arlt, T.; Klages, M.; Krüger, P.; Hartnig, C.; Scholta, J.; Müller, B. R.; Riesemeier, H., Combined synchrotron X-ray radiography and tomography study of water transport in gas diffusion layers. *Micro & Nano Letters* **2012,** *7*, 689-692.
[7] Arlt, T.; Manke, I.; Wippermann, K.; Tötzke, C.; Markötter, H.; Riesemeier, H.; Mergel, J.; Banhart, J., Investigation of the three-dimensional ruthenium distribution in fresh and aged membrane electrode assemblies with synchrotron X-ray absorption edge tomography. *Electrochemistry Communications* **2011,** *13*, 826-829.
[8] Arlt, T.; Klages, M.; Messserschmidt, M.; Riesemeier, H.; Scholta, J.; Banhart, J.; Manke, I., Influence of artificial aging of gas diffusion layers on the water management of PEM fuel cells. *ECS Electrochemistry Letters* **2014,** *3*, F7-F9.
[9] Netzeband, C.; Arlt, T.; Wippermann, K.; Lehnert, W.; Manke, I., Three-dimensional multiscale analysis of degradation of nano-and micro-structure in direct methanol fuel cell electrodes after methanol starvation. *Journal of Power Sources* **2016,** *327*, 481-487.
[10] Hinebaugh, J.; Lee, J.; Mascarenhas, C.; Bazylak, A., Quantifying Percolation Events in PEM Fuel Cell Using Synchrotron Radiography. *Electrochimica Acta* **2015,** *184*, 417-426.
[11] Lee, J.; Chevalier, S.; Banerjee, R.; Antonacci, P.; Ge, N.; Yip, R.; Kotaka, T.; Tabuchi, Y.; Bazylak, A., Investigating the effects of gas diffusion layer substrate thickness on polymer electrolyte membrane fuel cell performance via synchrotron X-ray radiography. *Electrochimica Acta* **2017,** *236*, 161-170.
[12] Lubetkin, S., The fundamentals of bubble evolution. *Chemical Society Reviews* **1995,** *24*, 243-250.

[13] Chen, Q.; Luo, L.; White, H. S., Electrochemical generation of a hydrogen bubble at a recessed platinum nanopore electrode. *Langmuir* **2015,** *31*, 4573-4581.
[14] Ahn, S. H.; Choi, I.; Park, H.-Y.; Hwang, S. J.; Yoo, S. J.; Cho, E.; Kim, H.-J.; Henkensmeier, D.; Nam, S. W.; Kim, S.-K., Effect of morphology of electrodeposited Ni catalysts on the behavior of bubbles generated during the oxygen evolution reaction in alkaline water electrolysis. *Chemical communications* **2013,** *49*, 9323-9325.
[15] Whitney, G. M.; Tobias, C. W., Mass-transfer effects of bubble streams rising near vertical electrodes. *AIChE journal* **1988,** *34*, 1981-1995.
[16] Burgmann, S.; Blank, M.; Panchenko, O.; Wartmann, J., µPIV measurements of two-phase flows of an operated direct methanol fuel cell. *Experiments in fluids* **2013,** *54*, 1513.
[17] Lee, J.; Hinebaugh, J.; Bazylak, A., Synchrotron X-ray radiographic investigations of liquid water transport behavior in a PEMFC with MPL-coated GDLs. *Journal of power sources* **2013,** *227*, 123-130.
[18] Borup, R.; Meyers, J.; Pivovar, B.; Kim, Y. S.; Mukundan, R.; Garland, N.; Myers, D.; Wilson, M.; Garzon, F.; Wood, D., Scientific aspects of polymer electrolyte fuel cell durability and degradation. *Chemical reviews* **2007,** *107*, 3904-3951.
[19] Rakousky, C.; Reimer, U.; Wippermann, K.; Carmo, M.; Lueke, W.; Stolten, D., An analysis of degradation phenomena in polymer electrolyte membrane water electrolysis. *Journal of Power Sources* **2016,** *326*, 120-128.
[20] Cherevko, S.; Topalov, A. A.; Zeradjanin, A. R.; Keeley, G. P.; Mayrhofer, K. J., Temperature-dependent dissolution of polycrystalline platinum in sulfuric acid electrolyte. *Electrocatalysis* **2014,** *5*, 235-240.
[21] Laconti, A.; Liu, H.; Mittelsteadt, C.; McDonald, R., Polymer electrolyte membrane degradation mechanisms in fuel cells-findings over the past 30 years and comparison with electrolyzers. *ECS Transactions* **2006,** *1*, 199-219.
[22] Grigoriev, S.; Dzhus, K.; Bessarabov, D.; Millet, P., Failure of PEM water electrolysis cells: Case study involving anode dissolution and membrane thinning. *International Journal of Hydrogen Energy* **2014,** *39*, 20440-20446.
[23] Debe, M.; Hendricks, S.; Vernstrom, G.; Meyers, M.; Brostrom, M.; Stephens, M.; Chan, Q.; Willey, J.; Hamden, M.; Mittelsteadt, C. K., Initial performance and durability of ultra-low loaded NSTF electrodes for PEM electrolyzers. *Journal of the Electrochemical Society* **2012,** *159*, K165-K176.
[24] Feng, Q.; Yuan, X. Z.; Liu, G.; Wei, B.; Zhang, Z.; Li, H.; Wang, H., A review of proton exchange membrane water electrolysis on degradation mechanisms and mitigation strategies. *Journal of Power Sources* **2017,** *366*, 33-55.
[25] Panchenko, O.; Borgardt, E.; Zwaygardt, W.; Hackemüller, F. J.; Bram, M.; Kardjilov, N.; Arlt, T.; Manke, I.; Müller, M.; Stolten, D.; Lehnert, W., In-situ two-phase flow investigation of different porous transport layer for a polymer electrolyte membrane (PEM) electrolyzer with neutron spectroscopy. *Journal of Power Sources* **2018,** *390*, 108-115.
[26] Hussey, D. S.; LaManna, J. M.; Baltic, E.; Jacobson, D. L., Neutron imaging detector with 2 µm spatial resolution based on event reconstruction of neutron capture in gadolinium oxysulfide scintillators. *Nuclear Instruments and Methods in Physics Research Section A: Accelerators, Spectrometers, Detectors and Associated Equipment* **2017,** *866*, 9-12.
[27] Görner, W.; Hentschel, M.; Müller, B.; Riesemeier, H.; Krumrey, M.; Ulm, G.; Diete, W.; Klein, U.; Frahm, R., BAMline: the first hard X-ray beamline at BESSY II. *Nuclear Instruments and Methods in Physics Research Section A: Accelerators, Spectrometers, Detectors and Associated Equipment* **2001,** *467*, 703-706.
[28] Li, X.; Yortsos, Y., Visualization and simulation of bubble growth in pore networks. *AIChE Journal* **1995,** *41*, 214-222.

Figure Captions

Figure.1: Schematic cell construction: a) view of the cell from the beam direction; b) lateral view of the cell; c) two PTL are contacted with the edge to a CCM, with the synchrotron beam, the central area is visualized.

Figure. 2: a: original image ; b: cutout cathode, normalized image, only the structures that have changed their position are visible (gas bubbles and catalyst particles); c-e: cutout pore network. The radiograph series shows the growth and propagation of hydrogen bubbles in the pores of the PTL at 0.1 A cm^{-2}.

Figure 3: a–e: Synchrotron radiographs showing the change and thinning of the catalyst layer.

Figure 4: Post mortem EDX analysis of the titanium HDH sample: a) distribution of chemical elements; b)Ir distribution; c) Pt distribution.

Figure 5: Polarization plots at ambient temperature and different flow rates.

Figure 6: Pore radius distribution measured with ~~M~~mercury porosity measurements.

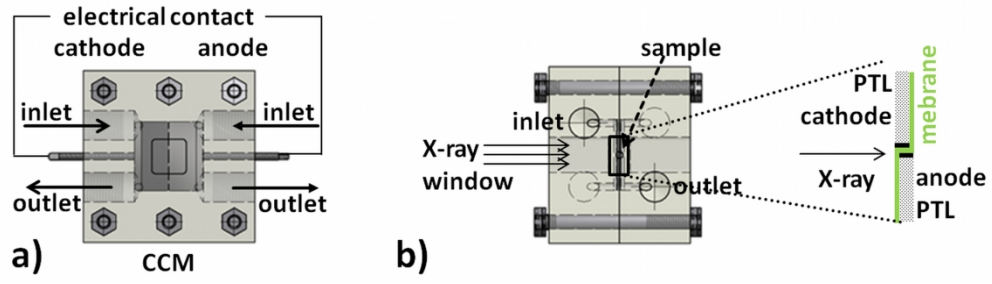

Figure.1: Schematic cell construction: a) view of the cell from the beam direction; b) lateral view of the cell; c) two PTL are contacted with the edge to a CCM, with the synchrotron beam, the central area is visualized.

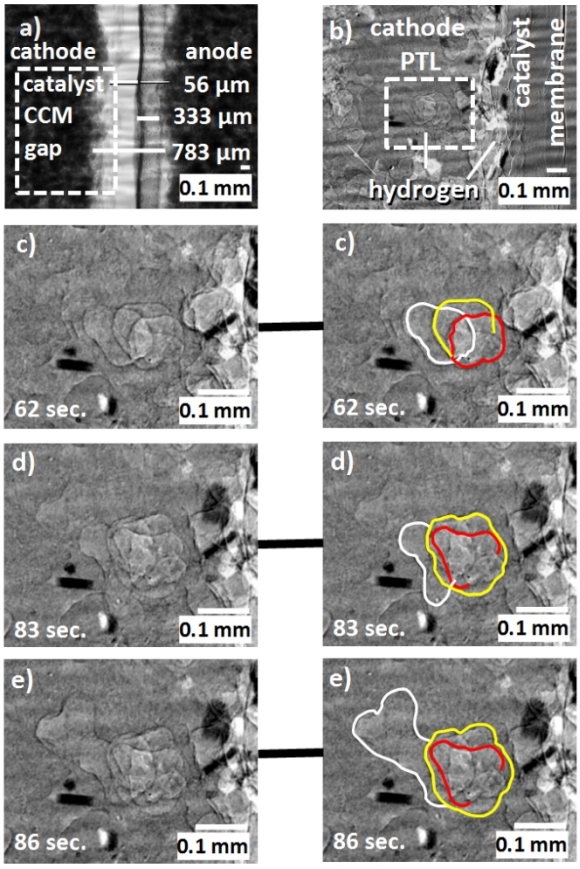

Figure. 2: a: original image ; b: cutout cathode, normalized image, only the structures that have changed their position are visible (gas bubbles and catalyst particles); c-e: cutout pore network. The radiograph series shows the growth and propagation of hydrogen bubbles in the pores of the PTL at 0.1 A cm-2.

25196x35636mm (1 x 1 DPI)

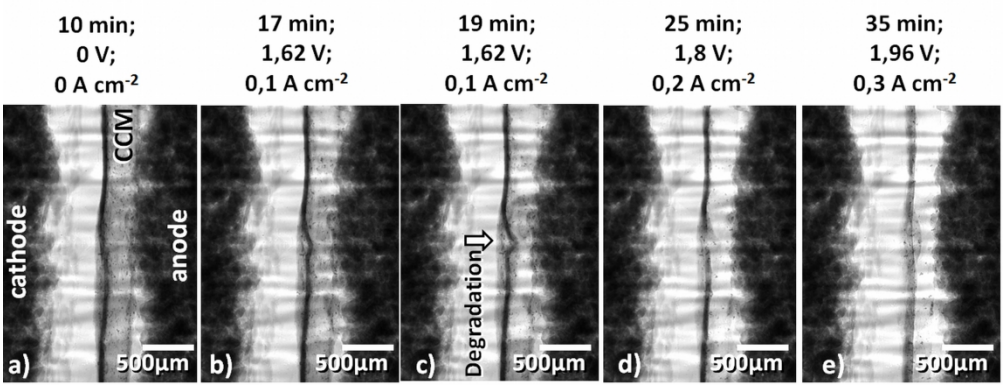

Figure 3: a-e) Synchrotron radiographs showing the change and thinning of the catalyst layer.

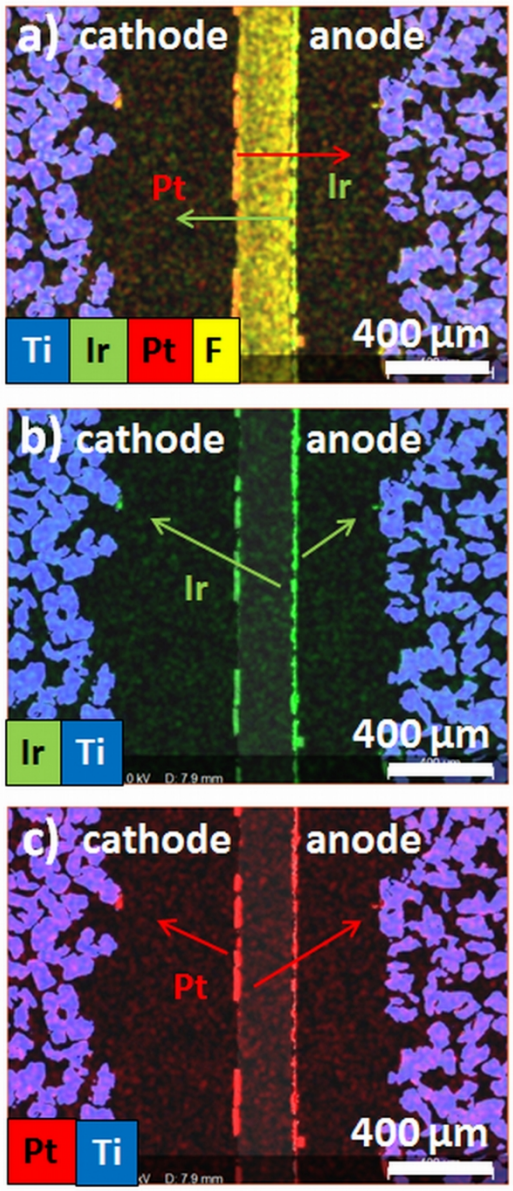

Figure 4: Post mortem EDX analysis of the titanium HDH sample: a) distribution of chemical elements; b) Ir distribution; c) Pt distribution.

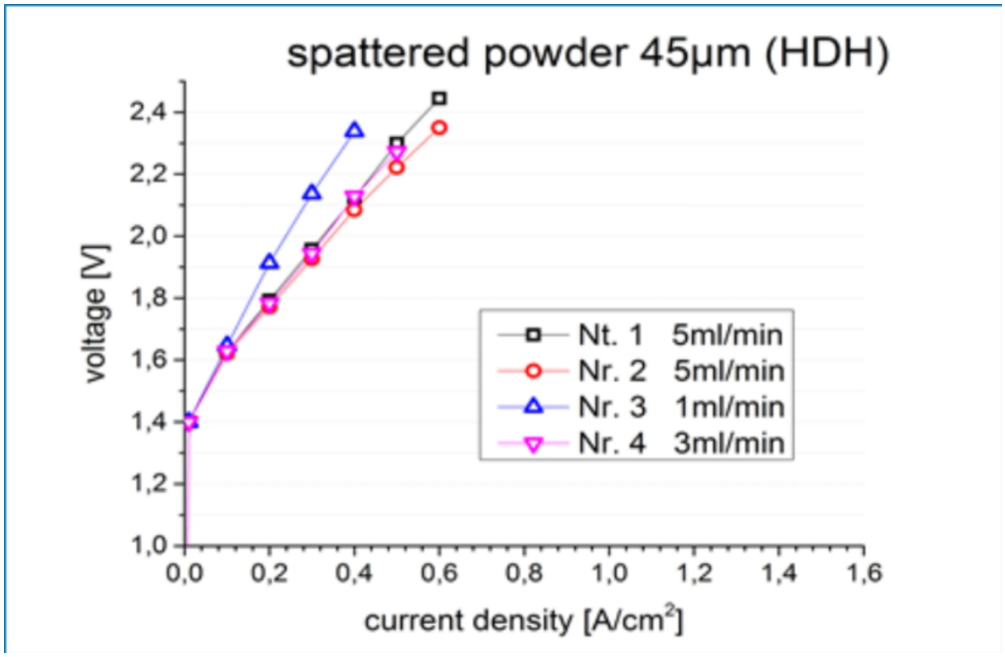

Figure 5: Polarization plots at ambient temperature and different flow rates.

38100x24688mm (1 x 1 DPI)

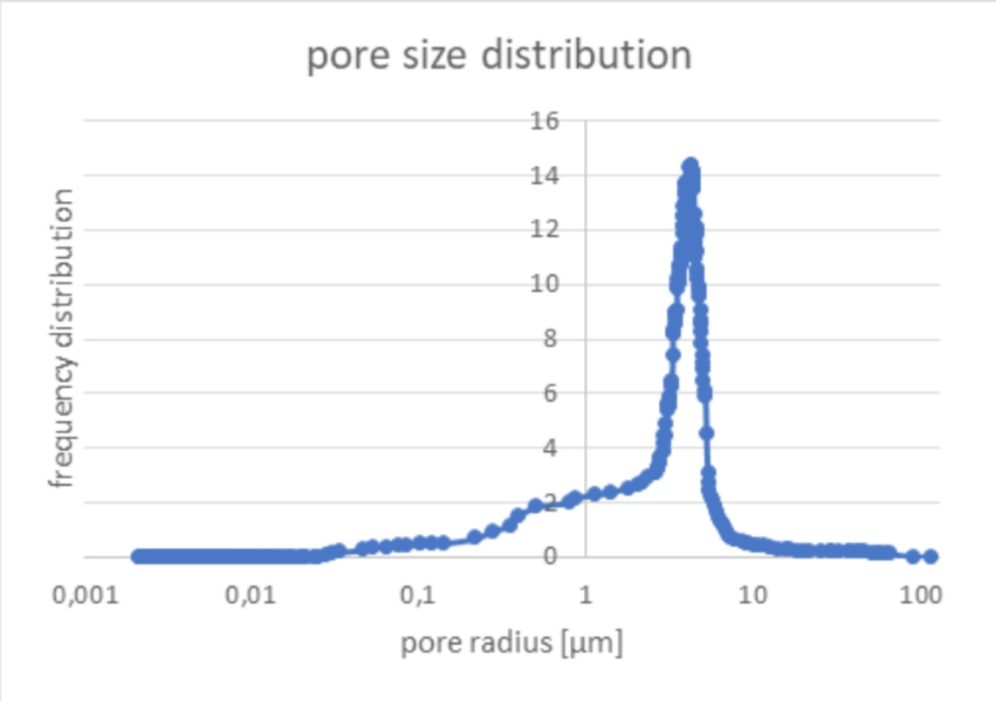

Figure 6: Pore radius distribution measured with mercury porosity measurements.

38125x26746mm (1 x 1 DPI)

Dear Reviewers,

Thank you very much for your feedback and for giving us the chance for further improving the text. According to your suggestions, we have reworked the article and hope now it will be acceptable for publication.

Best regards
Martin Müller

Reviewer: 3

Recommendation: Major Revision

Comments:
The authors have significantly improved overall readability of the manuscript. Several major technical issues still remain that were not properly address from the first review.

In Section 3.2 – You state that you observed the cell during humidification and operation and catalyst removal only occurred during operation, you use this to justify exclusion of beam damage. How long was the cell observed during humidification and operation? Were these equal amounts of time? Did you try different time windows to determine if dose had an effect?

The humidification of cells lasted 30 minutes and the total operating time was around 20 hours. This effect, that the visible degradation only begins with cell operation, was also observed in another test (and other cell construction) in the measurement in Berlin (Ber II neutron radiation). These tests were carried out in Berlin (Bessy II synchrotron radiation) and we had only 3 days of measurement, we did not have the opportunity to test the different proportions of moistening and operating time. As a rule, you get the opportunity to carry out the measuring campaign in Berlin once or twice a year. However, your hint to test different time windows would be very important to clarify this point in further experiments.

Reviewer 1 comment regarding catalyst movement (p23, line 55) – Can you provide the plot for the mercury porosimetry? I would like to better understand the amount of large connected porosity. I find it very suspicious that a 70 micrometer particle could move into the PTL as far as it did.

Pore radius is logarithmic normal distributed with the peak at 6 µm and a Full Width at Half Maximum (FWHM) of 4 µm.

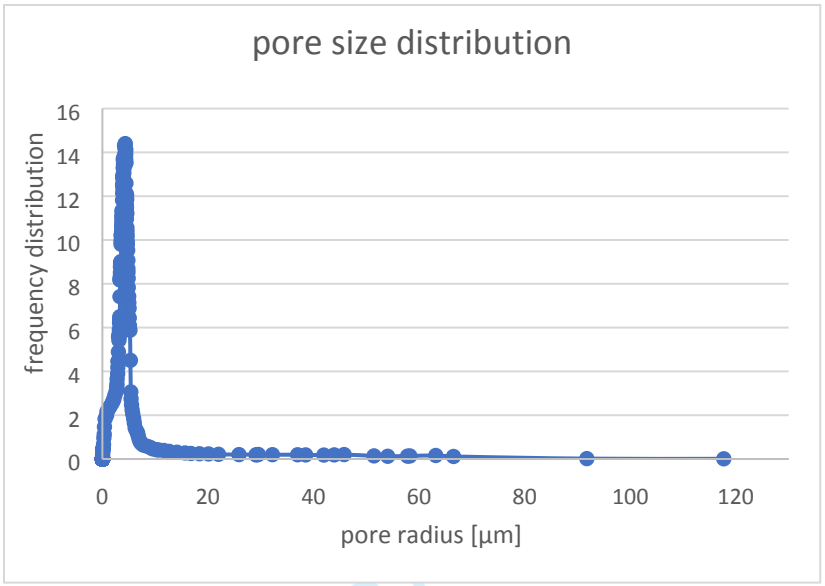

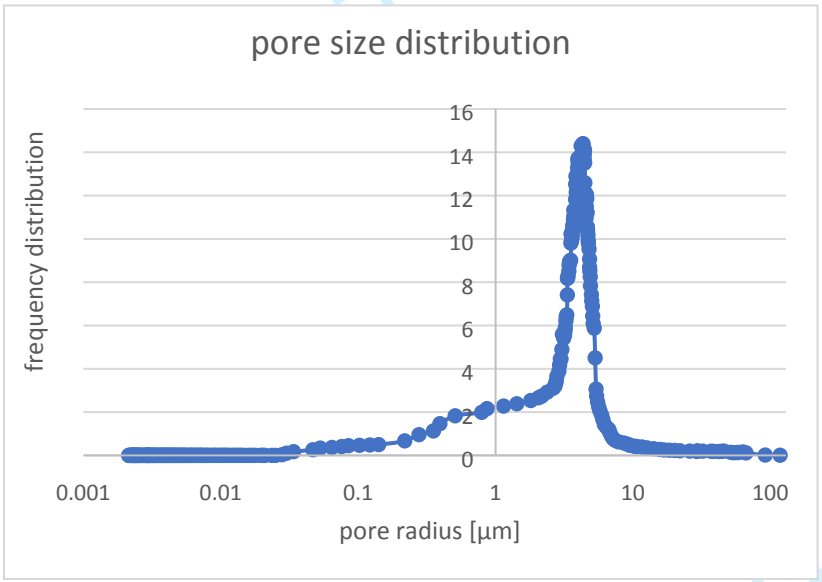

Response to Reviewer 2, item 10 – How is it possible to resolve 500 nm objects when the pixel pitch of the camera is 500 nm? Based on the Nyquist sampling theorem, you need a minimum of 2 pixels to resolve an object. This would put your best-case resolution at 1 micrometer. Real resolution will most likely be worse than this due to things like scatter and attenuation. You go on to further state that the resolution was proven in another article. Please provide details on this. If it was measured with a Siemens star that would be the resolution at the scintillator not the real image resolution. The cell hardware has a strong influence on real resolution.

The specified resolution was measured with Siemens Star, that's why it is also in the text: “Structures of few µm in size can indeed be distinguished.” → text is modified.

Response to Reviewer 2, item 11 – Your response to the question regarding the poor transmission is not satisfactory. The beam transmission through this thickness of material is too low to be of use. All results inside the PTL are suspect. Given the thickness, you state for the PTL in the beam direction and its porosity, the layer is basically opaque. You typically would need ~30% transmission to do anything quantitative and you have below 1% transmission.

You are right, the transmission is indeed low. With original images without editing we cannot see the bubble structures. We used methods that come from astrophysics for image processing. Since it's about the "change" of the state, you can indeed visualize everything very well. The pictures show the processes, but you can see even better if you combine the pictures in a video. These videos were presented at the conference presentation.

Response to Reviewer 2 – Reviewer 2 asked why neutron imaging was not considered and you responded that the resolution obtainable with neutrons is too low. Please be aware that NIST has demonstrated a detector capable of 1.5 micrometer resolution for fuel cell imaging, https://doi.org/10.1016/j.nima.2017.05.035. The neutron imaging facilities at PSI also have a microscope setup showing neutron resolution in the ~5 micrometer range. The resolutions of these two systems are on the same level or better than what you are getting with X-rays and would have orders of magnitude more transmission through titanium. Please discuss this decision.

Thanks for pointing out, when comparing neutrons and synchrotron radiography, we referred to facilities in Berlin (Ber II and Bessy II). We have good cooperation with colleagues in Berlin and have so far only measured there. Of course, other systems can be better. We will inform ourselves about the other possibilities.

We have added the following sentence into the article → As we have already performed tests with neutron radiography at the beamline at Helmholtz Center Berlin [24] we have found that the spatial resolution of this device is limited to around 6.3 µm. We also now about the higher resolution of other neutron sources, for an example up to 1.5 µm at the NIST [25] but due to the limited availability in this study, synchrotron X-ray radiographic imaging was employed to dynamically visualize the bubble formation and catalyst degradation.

The EDX results – Is this the same area as imaged with X-rays? Was the material removed from the cell? Is it actually representative of what was seen in the imaging experiments? If it was removed from the cell used for imaging how what the material compression maintained so as to not disturb anything?

The EDX shows the same range only of course with different resolution. After operation due to the contact pressure, the MEA was firmly connected. It was very easy to remove MEA from the cell with tweezers and embed it. After embedding, the parts were exposed to no mechanical or other stress. With the polisher it was possible to examine very well the sample internal structure. We ran the sample to half thickness and made EDX so that the elements in PTL pores could be analyzed.

Response to reviewer 2, item 16 – Even if the performance is poor you could still provide a pol curve to help the reader to understand what was the limiting factor in performance. Was it ohmic? Transport?

The polarization curves shown in the figure below. We decided not to include any polarization curves in the paper because it is not in focus. In the text it is described, that we could go only up to 0.6 A/cm^2, because the tension was already over 2.2 V. Otherwise, the curves show no abnormalities. The paper already contains a lot of information on different topics and we do not want to overload it, but we included the polarization plot now into the text.

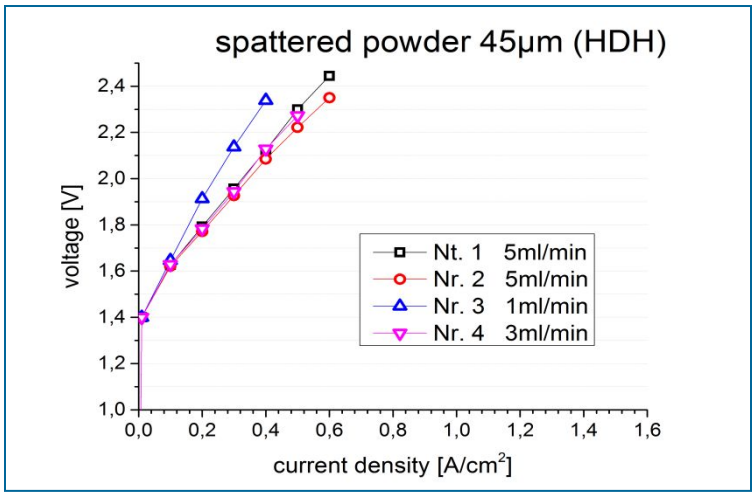

Response to reviewer 3, item 4 – That is correct, you normally would not have a gap. But in your case there appears to be one. Even with the correction made to the thicknesses of the MEA there is still too much distance between the PTLs. You claim that the PTLs must make contact as there if electrical conductivity. Is it possible that the area imaged has a gap and the electrical contact is made in another location? Could this gap, if it exists be the cause of the extensive, accelerated catalyst degradation?

Has any consideration been given to the quality of the alignment of the cell? The distance between PTLs is still discrepant with the thickness stated for the membrane and catalyst layers. Either the cell was misaligned with the beam or a gap existed between the PTL(s) and the catalyst layer(s).

That's exactly what we meant. The mapped area randomly shows a gap, and contact was made through another location (not visible in the picture). The visible distance between PLT and CCM is around 400µm. In every manufacturing process of bipolar plates, there is a certain surface roughness and surface waviness. The same applies to cutting PTL. It was cut with a jet of water so that the pores on the edge are not sealed. This creates a fault tolerance. The gap was not caused by the degradation, as it was also observed during humidification.

Remarks included in the pdf file

There are a number of assertions and discussion made in the text which are not backed up by results or references to other works. Of particular concern is that:

1. No polarization curve is shown despite being referred to in page 10.
   Is now included in the document.

2. No porosimetry data is shown despite being referred to in page 11.
   Is now included in the document.

3. No images of gas bubbles at higher current densities are shown despite being referred to in page 11.
   We decided not to include these pictures as we already have many pictures included.

4. It was stated that structures of a 0.5 µm in size can be distinguished by the imaging setup. The authors, in response to previous comments, stated that other works showed this, but these works are not referenced in the text.
We have added these references into the text: As we have already performed tests with neutron radiography at the beamline at Helmholtz Center Berlin [24] we have found that the spatial resolution of this device is limited to around 6.3 µm. We also now about the higher resolution of other neutron sources, for an example up to 1.5 µm at the NIST [25] but due to the limited availability in this study, synchrotron X-ray radiographic imaging was employed to dynamically visualize the bubble formation and catalyst degradation.

Other comments on the revised text:
5. Pg 3 line 40: "The investigation of blistering becomes difficult as it takes place in a porous medium". This sentence seems out of context and there is no explanation of blistering or previous attempts to investigate it. Is this blistering of the catalyst layer, of the membrane etc.? Please elaborate.
Sentence is reworked.

6. Pg 5 line 17: The reference used (18) refers to this oxide formation process taking place at the cathode of a fuel cell and not the cathode of a water electrolyzer where the thermodynamic conditions are very different and it is unlikely that oxide formation occurs. Other references refer to the processes in electrolyzer catalyst degradation such as
https://doi.org/10.1016/j.jpowsour.2016.06.082.
Is modified to: In case of fuel cells this is caused by oxide formation and oxide reduction along with molecular oxygen evolution in addition to the Platinum dissolution [18]. In PEM electrolysis additional degradation processes occur, the increase of contact resistance and the associated loss of performance is described in [19] and on the other hand particle agglomeration known as Ostwald ripening, causes agglomerates to grow larger, as small agglomerates get smaller and disappears [20].

7. Pg 10 line 2: should read figure 2(a).
Is modified, thanks.

8. Pg 10 line 17: The polarization curves are not shown. Please include them in the paper if you are going to refer to them. If there is not room in the text they should be included as a supplemental. The performance of the cell is not the primary concern of the article but it would be helpful to evaluate the performance of the cell alongside the visualization data.
Is now included.

9. Pg 10 line 22: Please add some dimensions to figure 1 or a reference coordinate system (x,y,z) in order to demonstrate to the reader which surface/length is being referred to here.
Dimensions are included.

10. Pg. 19 figure 2(a). This is still quite confusingly labelled. Maybe try using arrows or similar to refer to points of interest.
Is now modified.

11. Pg 10 line 56: These are quite large and regularly shaped agglomerations of Pt/C particles. A typical Pt/C particle is ~100 nm and these agglomerations must therefore be very big compared to those observed in the literature. How was it confirmed that these are Pt/C? Are there any other possible explanations?

There are also many small agglomerates to be seen, only the largest are up to 100 µm in size. The size of aglomerates could be determined through the decal process. Structures form after the decal process and during drying. The structures may detach completely from the substrate.

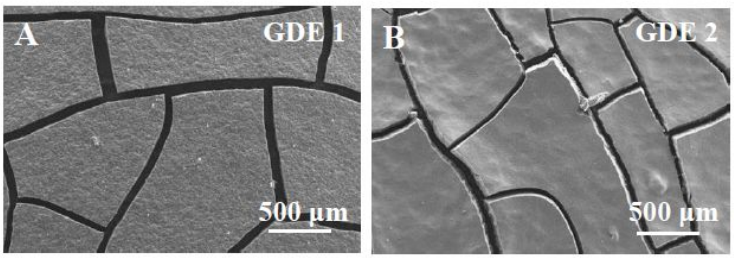

Image from Shuai Liu's dissertation "Morphology and Degradation of High Temperature Polymer Electrolyte Fuel Cell Electrodes"

12. Pg 10 Line 60: Please refer to figure 2(c).
Is changed.

13. Pg 11 line 3: If each image took 2 seconds to collect, would you expect there to be a significant growth/change of position of the bubbles during this time?
As the current densities are relatively low, we do not expect fast changes.

14. Pg 11 line 11: Please include the mercury porosimetry data if not in the main paper, then in a supplemental. It is not good practise to refer to results in the text that are not presented and can't be evaluated by the reader.
We will integrate these data.

15. Pg 11 line 12: Can you please estimate the actual percentage of 'big pores' in the PTL? You should be able to integrate the area under the porosimetry curve for the pore size range you refer to.

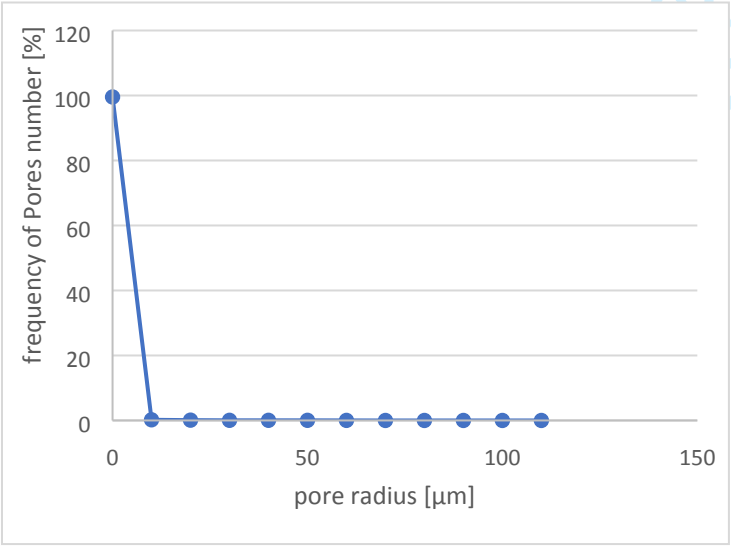

Only 0.5% of all pores are larger than 10 µm. But if you look at pore volumes, 0.5% pores make up 99.6% of all pore volumes. As an example, there are only 0.0006% of pores around 100 µm in size, but they form almost 40% pore volume. For the volume calculation it was assumed that the pores have a spherical shape.

pore radius [µm]	frequency of pores number [%]	volume fraction [%]
0	99,543	0,341

10	0,207	0,562
20	0,096	2,672
30	0,045	3,375
40	0,044	6,090
50	0,042	16,385
60	0,021	13,067
70	0,000	0,000
80	0,000	0,000
90	0,001	18,488
100	0,000	0,000
110	0,001	39,020

16. Pg 11 line 15: Do you have an estimate of the hydrophilicity (drop shape analysis etc.) of the PTL material? Were any procedures carried out to enhance the hydrophilicity? Is the bubble transport through the PTL expected to be capillary force dominated or dominated by viscous forces?
The behavior in this case depends not only on the pore structure, but on the oxide layer that forms on the titanium structure. The longer the cell was in operation, the larger the oxide layer could be detected, the more hydrophilic the structure. The area is currently under investigation and no definite conclusions can be drawn yet.

17. Pg 11 line 17: Give that the pixel resolution is 0.5 um, it should be possible to resolve structures of >1.5 um (3 pixels) in size. A 6 um pore would have a diameter of 12 pixels (~112 pixel area) which should be relatively easy to resolve. It is much more likely that there is insufficient intensity difference between the gas filled and water filled pores of that size that will distinguish them from the noise. If you know the magnitude of the noise in your setup it should be relatively trivial to calculate the lower bound of the bubble size that can be distinguished. Adjusting the energy of the beam to maximise the absorption difference between the water/hydrogen should allow you to image smaller bubbles.
Thanks for the suggestion and your opinion, we will consider it in the next measurements.

18. Pg 11 line 27: Again, no images are shown for the bubble movement at higher current densities. If this is stated in the text it should be supported by images/graphs or other information as opposed to assertions. This was requested in the previous review but not included. Videos mentioned in response to the previous comment on this topic could be included online or in supplementary material and would be of great interest and help to the reader.
Thanks for the suggestion and your opinion, we will consider it in the next measurements. We will upload the videos.

19. Pg 12 line 15: Degradation from the beam can take some time to occur, as it is dose-related. While this observation makes it less-likely that the initial degradation was beam-related, it does not exclude the possibility of beam damage to the sample or the possibility of damage to the ionomer in the catalyst layer allowing for easier detachment of catalyst particles by bubble formation etc.
Maybe this had accelerated the degradation?

20. Pg 12 line 31: Particle movement in figures 3 (a-e) is not obvious from the sequence of images and appears there is even a decrease in the number of particles observed from (a-e). Is it possible to highlight the particle movement or show a zoomed in image of the particle movement?
Unfortunately, we cannot provide these data.

21. Pg 12 line 33 and line 38: Which catalyst layer (anode or cathode) is being referred to?
It is the anode catalyst layer. Degradation at the cathode is negligible.

22. Pg 12 line 45: It was stated in section 3.1 that the cathode PTL was not in contact with the CCM. In this case the electrochemical reactions on the cathode (and possibly the anode) should proceed very slowly via lateral electrical contact in the catalyst layer. Is this degradation mechanism therefore representative of what happens in a real cell? Is there a possibility of mechanical detachment of particles from the layer due to ionomer swelling combined with the water flow?
It also seems that there is significant membrane thinning in the centre of the CCM at the cathode side in figures 3(b-e) (at the arrow location in fig. 3c). Is this caused by the lack of PTL contact to the CCM?
We think this is not a membrane thinning but probably your idea of a local lack of contact pressure in some areas is right.

23. P12 line 52: Is this the anode or cathode side? It is very difficult to see any distinct catalyst particles in the anode PTL and the channel is not shown so movement of particles to the channel cannot be verified.
Is now included in the sub headline that it is the anode.

24. Pg 12 line 60: Given that there is a lack on contact between the PTL and the CCM in figures 2 and 3 and that the seal completeness was not imaged, it is not inconceivable that there may be a gap in the seal.
We are sure that there is no gap within the sealant.

25. Pg 13 line 42: From looking at the images in figure 4, it does appear that there is some Ir(green) fig. 4(b) and Pt(red) fig. 4(c) in the membrane, in the area between the catalyst layer (Also, why is there such a large gap here?) and the PTL as well as within the TI particles of the PTL. Are these just noise from the EDX or is there PT and Ir present here? Is there a detection limit for the EDX you used? Grinding/polishing of CCM samples has also been known to spread materials of interest across the sample.
Yes, you are right, it could be noise. the EDX has a certain resolution, and the distribution of elements could also take place by polishing.

26. If catalyst migrated only through imperfections in the seal, then why is it mainly deposited on the surface of the CCM and not more evenly spread through the PTL?
Thanks for that hint.